

REPORT

The preparation of TiO₂ nanoparticles through hydrothermal phase transformation and its activity in water chemistry

Rafia Azmat*, Iqbal Altaf and Asma

Department of Chemistry, University of Karachi, Karachi, Pakistan

Abstract: The current article presents a simple new route of cost-effective and straight forward synthesis of the anatase structure of Titanium dioxide (TiO₂) nanoparticles (NPs). The solvent Hydrothermal Phase Transformed (HPT) method adopted for the conversion of bulk precursor of TiO₂ powder at Nano scale to get contaminated free photoactive TiO₂ NPs. The morphology, crystal phase and surface area characterization of NPs completed through scanning electron microscopy (SEM). The composition of elements in NPs determined through Energy Dispersive X-Ray Spectroscopy (EDS or EDX). The Fourier-transform infrared spectroscopy (FTIR) employed for molecular components and structures. Synthesized NPs showed 3D hexagonal pure anatase phase with size of 68 to 97 nm. The toxicity of TiO₂ NPs discovered on the water chemistry using two microbes like *Staphylococcus aureus* (*S. aureus*) and *Escherichia coli* (*E. coli*) and Acridine Orange (AO) by the dose-dependent manner followed by higher antimicrobial activities and degradation properties at shallow concentration in water respectively. The higher antimicrobial activities of 3D crystal structure related to its highest photo catalytic properties leading to membrane damage of microbes and mineralization of the dye. The recycled photo catalyst TiO₂ after 4 cycles retained the degradation efficiency of 75% against AO, subsequently concluded that the method of preparation was effective.

Keywords: TiO₂, 3D crystal structure, *Staphylococcus aureus* and *Escherichia coli*, acridine orange.

INTRODUCTION

Titanium being nontoxic widely used in paints, pigments and food to a small amount as well while titanium dioxide (TiO₂) nanoparticles (NPs) produced at bulk scale for industrial applications to encounter the ever-increasing market demands due to its unique chemical and physical properties (Zhang *et al.*, 2015). Due to the scarcity of delivering fresh drinking water, purification of water got an essential position in the field of research globally. Elimination of microorganisms, pollutants and toxins became an over-riding environmental issue (Lin *et al.*, 2008; Qadri *et al.*, 2009). For the sustained proper health care of the human, researchers highlighted on developing effective and inexpensive harmless reagents.

Bio effectiveness of particles can be improved by reducing the size and thus increase in the surface area (Kim *et al.*, 2007). Due to the tiny size and enhanced, modified properties, NPs found their application to remove pollutants from water. The water contaminated by numerous living and non-living matter where; with time microorganisms immune themselves to resist against various antibiotics. Furthermore; color persistent from dyes and paints increased the chemical oxygen demand (COD) (Pathakoti *et al.*, 2019). In the presence of these pollutants, water chemistry becomes more and more complicated. The maintenance of running stream requires

such an inexpensive active material, having both antimicrobials as well as degradative properties to grip the situation. Usually glycosaminoglycans, DNA, RNA, are stained through Acridine Orange, a metachromatic dye also used to analyze autophagy which at high dose denatures and precipitates both RNA and DNA. It enters into acidic organelles in a pH-dependent manner and usually discarded without further treatment.

The literature search revealed that the method of preparation, size and precursor enhanced the activities of the NPs in controlling the maximum pollutants from water. Lee *et al.*, (2008) also reported the antibacterial effects of Nano valent iron on *E. coli* and showed the relationship between *E. coli* suppression against NPs dosage. In Pakistan, most of the diseases caused by bacterial contamination of drinking water. World Health Organization (WHO) recommended for the drinking water that it should contain 0/100 mL of coliform or fecal bacteria. There is an urgent need to formulate a strategy to treat wastewater. Currently deployed techniques for the removal of bacteria and other contaminants from water are economically not feasible and require much care during their application.

The Nanotechnology displays a practical solution for controlling the pollutants present in water using various methods of synthesis of nano-materials. The aims and objectives of this article was to discuss the simple, cost-effective method of preparation of TiO₂ from its bulk

*Corresponding author: e-mail: rafiasaeed200@yahoo.com

precursor compound using ethanol as solvent followed by calcination. The characterization of prepared NPs conducted through SEM, EDX, IR and UV. The activity checked on two significant bacterial isolates where Acridine Orange (AO) selected due to its broader usage in medicinal as well as in the dye industry.

MATERIALS AND METHODS

Reagents

All of the chemicals were of analytical grade and used as received without further purification by employing demineralized water as preparatory medium. TiO_2 and Ethanol ($\text{C}_2\text{H}_5\text{OH}$) were obtained through Merck. All experiments were performed at ambient temperature ($25 \pm 2^\circ\text{C}$).

Synthesis of TiO_2 NPs

In a typical synthetic procedure 5 g TiO_2 , 20 mL ethanol ($\text{C}_2\text{H}_5\text{OH}$) and 280 mL of distilled water were added to a 500 mL Erlenmeyer flask. The mouth of flask was covered with aluminum foil which was punctured with few holes to avoid over pressure. This flask was then placed in an autoclave at 120-130 kPa (kilo Pascal) pressure for 12 hours at about 125°C . The obtained white precipitates were filtered through whatman no. 40 filter paper and washed with distilled water then dried in oven at 100°C for 4 hours. Obtained product was heated in furnace at 350°C for 4 hours.

Characterization of TiO_2 NPs

Samples were subjected for Scanning Electron Microscopy (JSM-6380A JEOL from Japan), Energy Dispersive X-ray Spectroscopy (EX-54175jMU JEOL from Japan) and Fourier Transform Infrared (Perkin-Elmer Inc Fourier transform infrared spectrophotometer) analysis.

Anti bacterial activity against *E. coli* and *S. aureus*

Antimicrobial activity of the prepared TiO_2 NPs was evaluated by microdilution method in 96 micro titre plate. Luria-Bertani (LB) broth was used for overnight growth of clinically isolated *S. aureus* and *E. coli*. 5×10^5 bacterial cells which were used as inoculum for each well except sterility control. TiO_2 NPs were dissolved in Dimethyl sulfoxide (DMSO) to achieve initial concentration of 1 mg/mL. All test and control wells were dispensed with 170 μL of LB broth followed by serial transfer of 170 μL of compound to achieve 2-fold serial dilutions in test wells of 96 micro titre plate except growth control well which contained cultures without compounds (table 1). Every test and control wells were then inoculated with 30 μL of inoculum and plates were incubated at 37°C for 24 hours. The whole experiment was carried out in triplicates to minimize and validate relative differences. Lowest concentration of compound showed no growth in test well, considered as minimum inhibitory concentration (MIC) and expressed in $\mu\text{g}/\text{mL}$ (table 2). Solutions of

different concentrations of TiO_2 were prepared (table 3) each with 100 mL tap water from local source and analyzed for finding the most probable number (MPN) of *E. coli* in water.

Degradation of Acridine Orange

The degradation of AO (fig. 1) was conducted by simple mixing of the 0.1 - 0.5 g of NPs with 50 mL solution of 250 ppm of the dye. The change in dye concentration was resolute quantitatively through quantifying absorbance using the filtered reaction solutions after every 10 minutes from reactor till clear solutions achieved. The samples were centrifuged to separate the TiO_2 catalyst for measuring the absorbance of the solutions. The absorbance of the dye was recorded after every 10 minutes using Shimadzu UV-1800A UV-Vis Spectrophotometer at $\lambda_{\text{max}} = 490 \text{ nm}$.

Efficiency of the decolorization system with time was calculated by equation 1.

$$\text{Decolourization efficiency} = \frac{A_0 - A_t}{A_0} \times 100 \text{-----(1)}$$

Where,

A_0 = initial absorbance

A_t = absorbance at time t

STATISTICAL ANALYSIS

After investigation of the experimental work, the data was subjected to Analysis of Variance (One-way ANOVA), using software SPSS 16 where the assays were performed in triplicate and the results stated by mean \pm SD (standard deviation) and significance considered with respect to experiments conducted without TiO_2 NPs.

RESULTS

The characterization and activities of NPs accompanied by using following advanced technologies.

Characterization of TiO_2 through SEM and EDS

The surface morphology, shape and the particle size of the synthesized Nanomaterial were inspected via a Quanta Inspect F scanning electron microscope (SEM). The sample was conducted at accelerating voltage of 15 kV in a vacuum coupled with the energy of electrons in a range from 0 to 20 keV for 30 sec real time. Nanomaterial of size as low as 68.8 nm to 97.0 nm were obtained as shown in fig. 2.

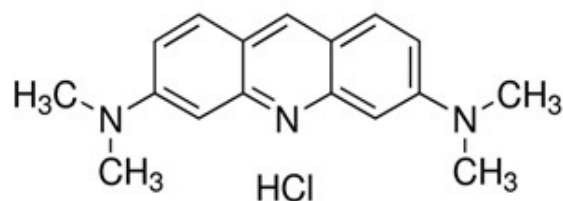


Fig. 1: Structure of acridine orange.

In conjunction with the analysis of surface morphology, the percent composition of synthesized NPs was examined through energy dispersive spectroscopy (EDS).

The EDS scan of the sample after calcination (fig. 3) showed the percentage composition as Ti is 36.08%, O is 57.37% and C is 6.56% (table 4).

Table 1: Tabular illustration of experimental scheme

Well no.	Concentration ($\mu\text{g/ml}$)	2 fold serial dilution	Inoculum (μl)
1	500	170 μl LB broth + 170 μl TiO ₂ (1mg/ml)	30
2	250	170	30
3	125	170	30
4	62.5	170	30
5	31.25	170	30
6	15.625	170	30
7	7.8	170	30
8	3.9	170	30
9	1.95	170	30
10	0.97	170 Discard	30
Sterility control	-	200	-
Growth control	-	170	30

Table 2: The Minimum Inhibitory Concentrations (MIC) of TiO₂ in $\mu\text{g/mL}$ against clinical isolate

TiO ₂ ($\mu\text{g/mL}$)	<i>E. coli</i>	<i>S. aureus</i>
TiO ₂	1.95 \pm 1.0**	1.95 \pm 1.0**

\pm Standard deviation of three replicates, double asterisks (**) represent highly significant differences ($P < 0.01$)

Table 3: *E. coli* detection at different concentrations of TiO₂

Concentration of TiO ₂ ($\mu\text{g/mL}$) in Sample + isolated <i>E. coli</i>	<i>E. coli</i> (MPN/100mL)
Control sample (Without TiO ₂)	+ ve
500	-ve
250	-ve
125	-ve
62.5	-ve
31.25	-ve
15.625	-ve
7.8	-ve
3.9	-ve
1.95	-ve
0.97	+ve

Table 4: EDS spectrum of synthesized TiO₂ Nanoparticles

ZAF Method Standardless Quantitative Analysis			
Fitting Coefficient: 0.3860			
Element	(keV)	mass%	At%
C K	0.277	2.89 \pm 0.5**	6.56 \pm 0.4**
O K	0.525	33.68 \pm 1.1**	57.37 \pm 1.0**
Ti K	4.508	63.43 \pm 2.1**	36.08 \pm 0.8**
Total		100	100

\pm Standard deviation of three replicates, Asterisks (*) represent significant differences ($P < 0.05$); double asterisks (**) represent highly significant differences ($P < 0.01$)

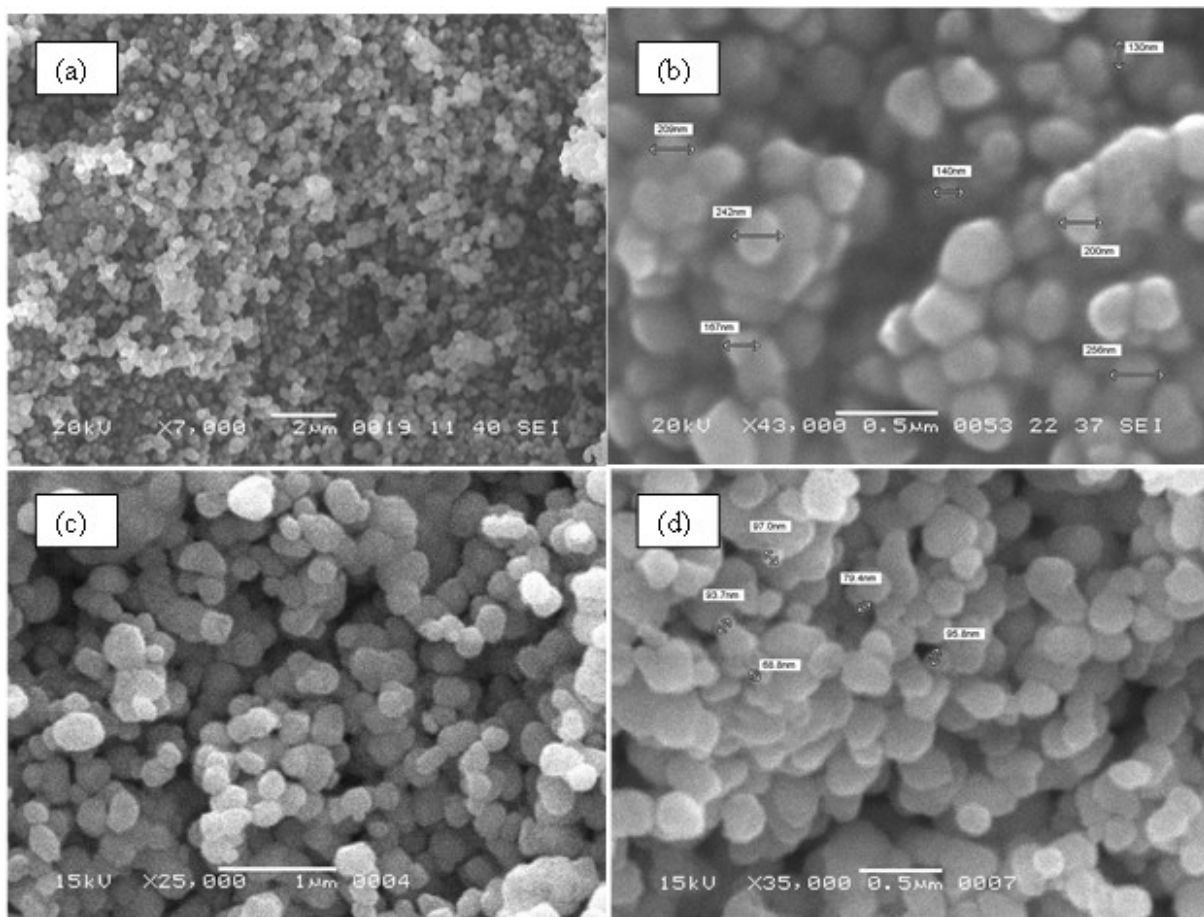


Fig. 2: Scanning Electron Microscopy images. (a) bulk TiO_2 , (b) synthesized TiO_2 Nanoparticles before calcination, (c) & (d) TiO_2 Nanoparticles after calcination showing hexagonal structures in which (d) is showing the exact particles size (68.8 nm to 97.0 nm)

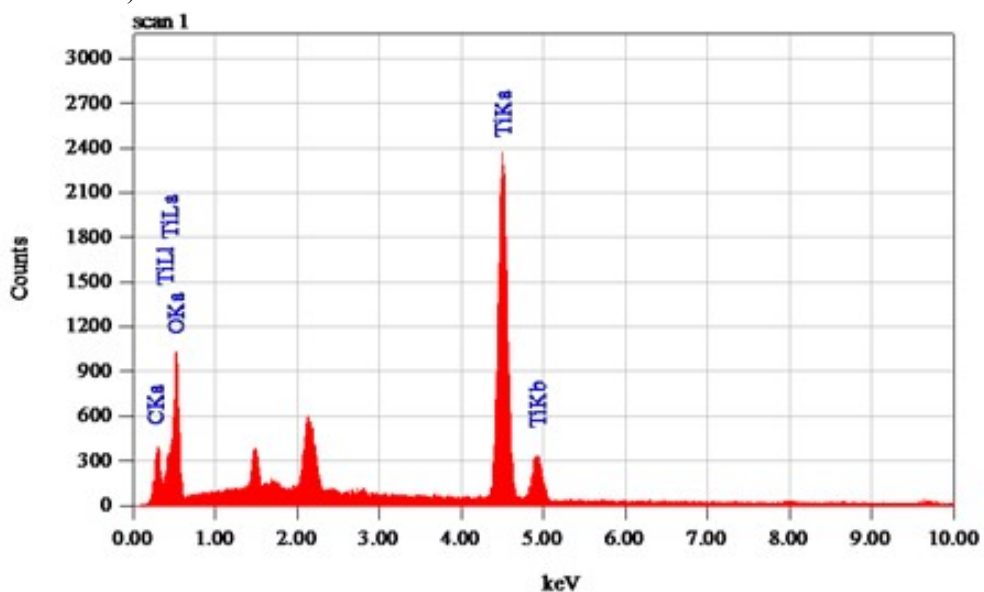


Fig. 3: Energy Dispersive X-ray Spectroscopy images of TiO_2 Nanoparticles particles after calcination

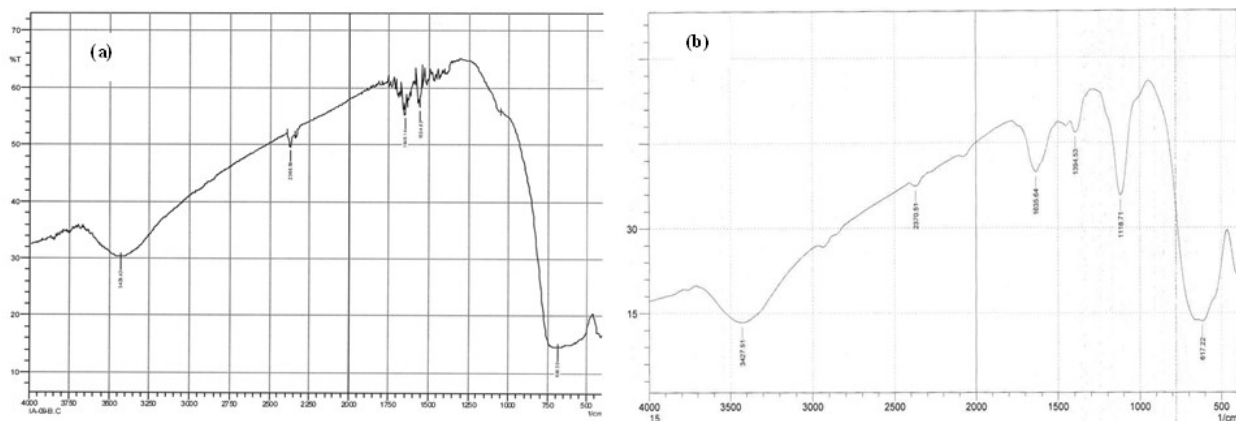


Fig. 4: Fourier Transform Infrared Spectroscopy images of TiO₂ Nanoparticles. (a) nanoparticles before calcination (b) nanoparticles after calcination

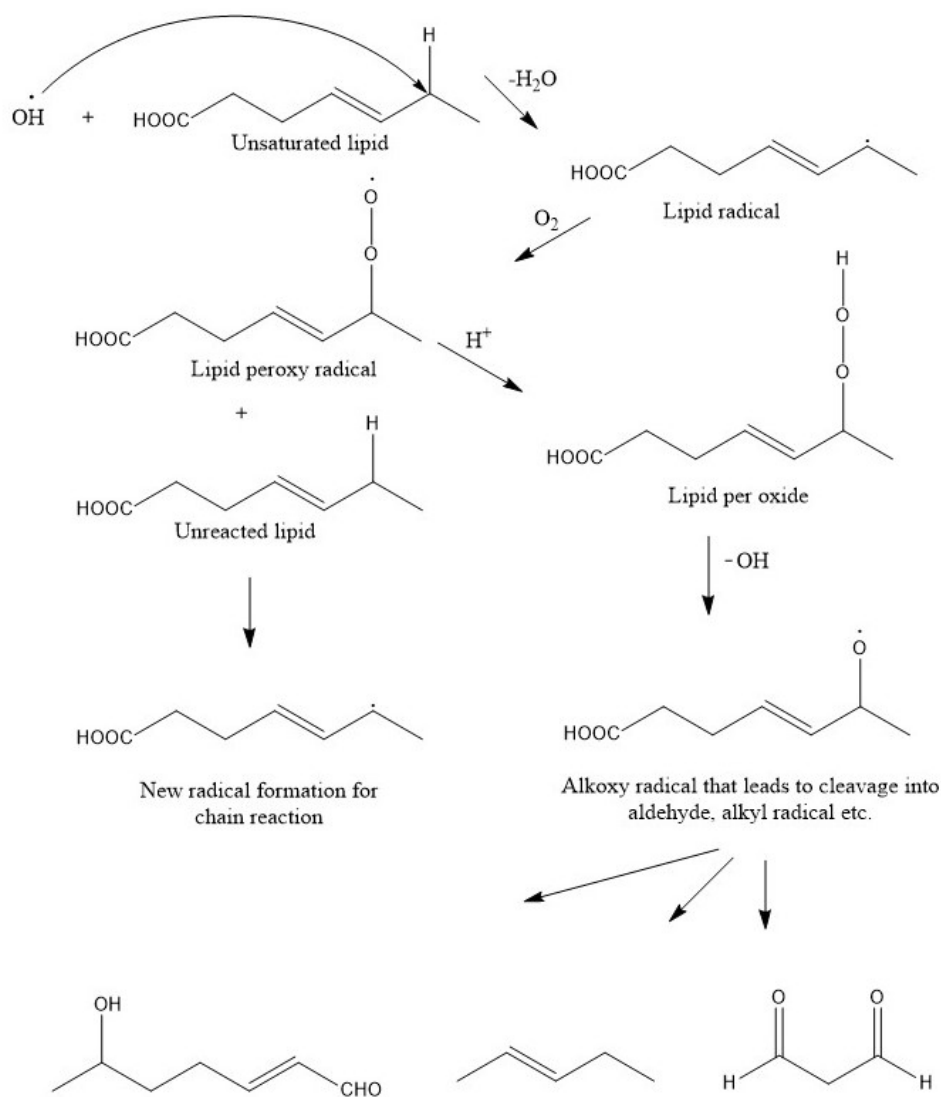


Fig. 5: Mechanism of oxidative destruction of cell wall (Lipid) of *E. coli* and *S. aureus*

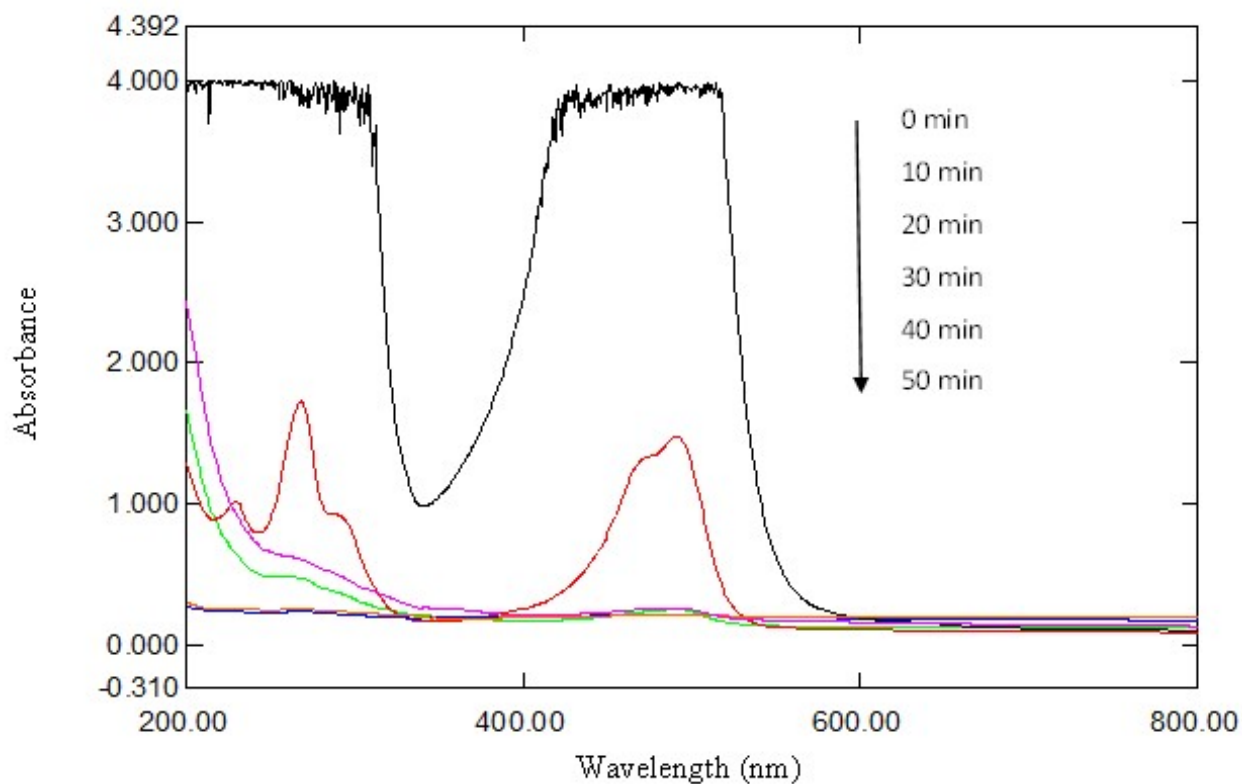


Fig. 6: Spectral changes of Acridine Orange (250 ppm) in presence of TiO_2 nanoparticles at different time interval.

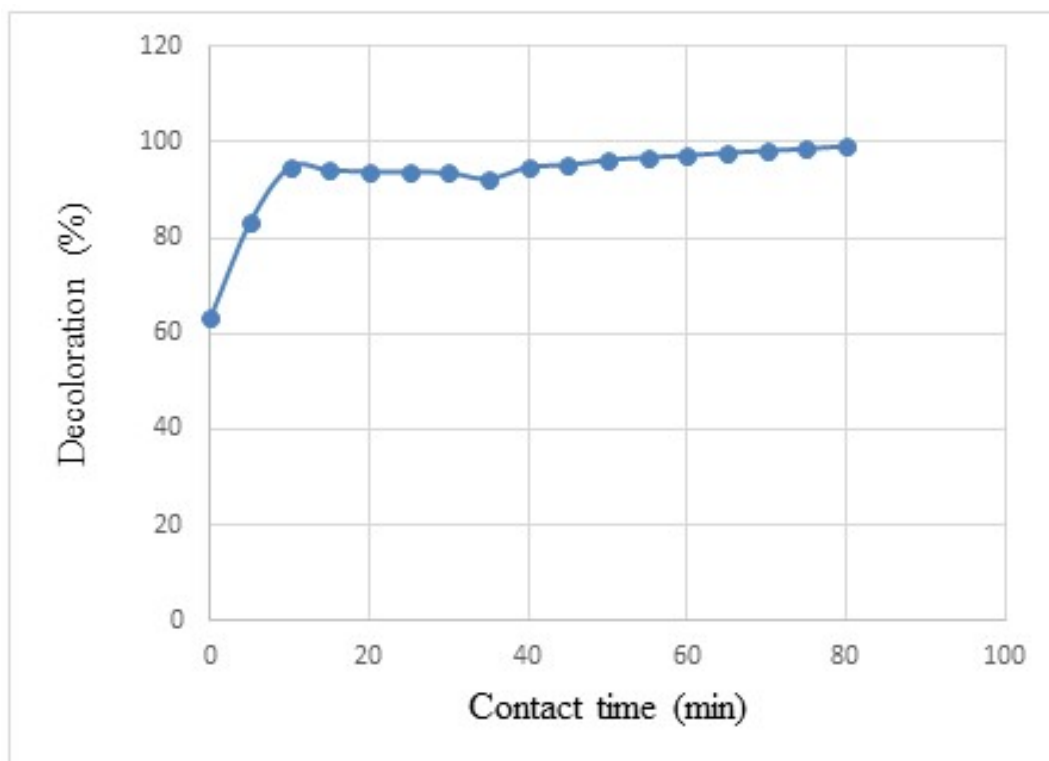


Fig. 7: Decolouration efficiency (%) of Acridine Orange with respect to contact time with TiO_2 nanoparticles

FTIR analysis

FTIR is modern quantitative tool for the analysis of functional groups and used to determine the nature of chemical bonding between atoms of phase transferred bulk at Nano Scale. FTIR spectra of prepared TiO₂ NPs shown in fig. 4 (a & b).

Antibacterial activity of TiO₂ NPs against *E. coli* and *S. aureus*

The activity of synthesized TiO₂ NPs was checked on two clinical isolates and in tap water samples as very diminutive information is available about the antibacterial activities of Titanium NPs and their action phenomenon.

In solutions of tap water, *E. coli* presence was found positive for control sample and for solutions less than 1.95 µg/mL TiO₂ NPs (table 3). For the solutions of 1.95 µg/mL and all greater concentrations of TiO₂ NPs, *E. coli* was found negative through MPN/100 mL method.

Degradation of Acridine Orange

The activity of as prepared, anatase TiO₂ NPs were checked against acridine orange (AO). The spectral changes of AO solution with the time, during the photo catalytic degradation process by TiO₂ presented in the fig. 6.

The decolourization of AO dye solutions in the presence of the TiO₂ NPs photo catalyst (0.0-0.5 g TiO₂/mL) studied as a function of contact time (fig. 7) where the decolourization of AO in the presence of TiO₂ NPs reached to 92.0% within 10 min with complete removal in 50 min.

DISCUSSION

Phase transformed solvent hydrothermal method for TiO₂ NPs

TiO₂ has been considered the most widely used oxide in photo catalysis, prepared by several methods including sol-gel, precipitation methods etc for degradation of organic compounds, reduction of inorganic ions and antibacterial activities etc. The present article discloses the new simple and cost effective method for synthesis of TiO₂ NPs due to its vast application at industrial scale. The synthetic process include modest phase transformed solvent hydrothermal method using TiO₂ bulk powder as precursor.

Characterization of TiO₂ through SEM and EDS

The ultrafine particles of material in the range of 1 – 100 nm size are called Nano-materials (Khan *et al.*, 2017). The image obtained through scanning electron microscopy showed the conversion of bulk TiO₂ into α-TiO₂ which is a most stable form of TiO₂ NPs and possess high anti-bacterial activities (Desai and Kowshik, 2009). The SEM images of the synthesized TiO₂ NPs showed in fig. 2(c - d) where the particle size ranged from

68.8 nm to 97.0 nm on a scale of 0.5 µm which was similar to the earlier reports of Khan *et al.*, (2017). The SEM images showed the pallets of hexagonal TiO₂ NPs after the aggregation (fig.2(b - d)). The SEM image of TiO₂ particles before calcination during the synthetic steps presented in fig. 2 (b) where the size of particles were in between 140 nm and 256 nm with no well-established morphology. It indicated from the images that calcination is a critical step of synthesis. It actually stores energy in the NPs that utilize later on during its application. The processes of calcination during preparation of Nanomaterials offer greatly improved nanostructure (68 to 97 nm) which enable the occupation of all intercalation sites available in the particle volume, leading to high specific capacities and make nanomaterial able, contributing a favourable solution for high-energy and high-power energy storage for several uses.

Bhatia (2016) reported that the size and morphology of synthesized NPs depends upon the type of method used for its synthesis. Mali *et al.*, (2013) investigated the conversion of TiO₂ at Nano-scale particles though hydrothermal technique at different temperatures where they observed variation in temperature, effect the morphology of synthesized Nano-material. Vijayalakshmi, & Rajendran (2012) synthesized TiO₂ NPs of size of ~100 nm by hydrothermal methods using NaOH. Rosi and Kalyanasundaram, (2018) synthesized TiO₂ NPs using *G. Cochinchinensis* leaf extract and observed the SEM within the magnification of 2 µm and 5 µm, the size was ranging from 15 nm to 45 nm.

EDS technique revealed the qualitative characterization data as atomic percentage (fig. 3, table 4). The percentage achieved in current investigation is found to be good in agreement of purity of TiO₂ NPs and similar to the previously experimented work of some researchers (Al-Harbi *et al.*, 2011; Peiris *et al.*, 2018). Extremely fine EDS analysis showed that investigated method of synthesis is free from contaminant, confirms the target atoms as well as the robustness of the synthetic procedure. Despite of being doubled in the ratio of Oxygen then Titanium the percentage composition of oxygen is greater than Ti but not two times due to the large size of Ti atom. Rosi and Kalyanasundaram, (2018) determined the elemental composition by EDX; confirmed that the NPs synthesized using *G. Cochinchinensis* leaf extract, indicates the amount of Titanium and Oxygen present in the TiO₂ NPs which were 84.02% & 15.98% respectively with no characteristic peaks of impurities or other precursor compounds as observed in current simple synthesis.

FTIR analysis of TiO₂

FTIR spectra of TiO₂ NPs shown in fig 4. The stretching absorption band of metals with oxygen falls between 800 cm⁻¹ to 400 cm⁻¹ (Ashiri, 2013). A strong absorption peak

at the wave number of 617.22 cm^{-1} in fig. 4 (b), reflects the characteristic peak of stretching between Titanium and Oxygen. The absorption peak of TiO_2 NPs differs dramatically as compared to the absorption wave number of TiO_2 in bulk (Al-Amin *et al.* 2016). The current work showed good agreement with the reported work of Rosi, & Kalyanasundaram (2018) where they detected the peaks analogous to the broad band centered at 543 cm^{-1} typical of Ti-O bending mode of vibration which confirms the formation of metal oxygen bonding. They also reported that the intense peak between 800 and 450 cm^{-1} describes the Ti-O stretching bands. The medium absorption peak in the FTIR spectra of TiO_2 NPs at 1118.71 cm^{-1} wave number corresponds to the stretching between two oxygen molecules which was similar to the work of (Das *et al.*, 2001).

The absorption of infra-red radiation by Oxygen-Oxygen stretching was absent in the FTIR spectrum of TiO_2 before calcination when compared with spectrum of after calcination NPs, (fig. 4a & 4b). It was observed that after calcination, particles became more energetic and peak of Oxygen-Oxygen (O-O) stretching enhanced in the IR spectrum. The intermolecular contact of water molecule with the surface of TiO_2 NPs contributed its presence in the spectra. The broad absorption peak at 3427.51 cm^{-1} is associated with the OH (hydroxyl) stretching of water molecule similar to broad band reported by Rosi and Kalyanasundaram (2018) between 3800 to 3000 cm^{-1} which is due to hydroxyl (O-H) stretch. The IR representing the water as moisture where weak absorption band at 1635.64 cm^{-1} belongs to the bending frequency of hydroxyl group (Al-Taweel and Saud, 2016).

Rosi and Kalyanasundaram, (2018) reported that the peak at 1676 cm^{-1} was related to O-H bending vibration of adsorbed water molecule on the surface of TiO_2 which may have critical role in photocatalytic activity of TiO_2 NPs.

Activity of TiO_2 NPs against *E. coli* and *S. aureus*

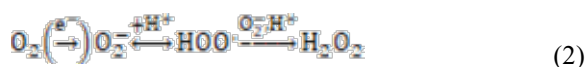
Gram positive and gram-negative bacteria are classified according to the cell membrane structure that consists mainly of peptidoglycan. *E. coli* being a gram-negative group, possess thinner peptidoglycan membrane between outer cell wall and the cytoplasmic membrane as compared to gram positive *S. aureus*. In current study antibacterial activities of NPs investigated in aerobic conditions in the natural environment. Because anaerobic or deaerated conditions are specially designed conditions and generally these bacteria produce diseases in natural environment that is aerobic. The hydrothermal phase transferred NPs showed complete growth inhibition effects at $1.95 \text{ }\mu\text{g/mL}$ for isolated *E. coli* and *S. aureus* (table 2) which reflects that Hydrothermal Phase Transformed (HPT) methods proves to have better efficiency. The detailed literature search reveals that TiO_2

affected in concentration range of 0.001 to 5000 ppm to inhibit bacterial growth which depends upon the particles size, wave length and strength of the UV light. While current study proves that TiO_2 NPs solution of $1.95 \text{ }\mu\text{g/mL}$ (ppm) has ability to complete inhibition of *E. coli* and *S. aureus* without using specific UV light in aerobic condition.

Due to the very small size and high reactivity NPs of Titanium accelerates the damaging the cell wall of the bacteria or binding to the chemical structure of the protein. Moreover, it is reported that the fundamental process of inhibition of bacteria *E. coli* and *S. Aureus* is not completely understood. The mechanism mode of the NPs on *E. coli* and *S. Aureus* are based on hypothesis that

- i) the DNA structure may be lost due to attack of reactive oxygen species (ROS) of TiO_2 NPs (Morones *et al.*, 2005).
- ii) Lin *et al.*, (2014) proposed that the cell wall of bacteria may be directly damaged due to the disturbing structure of protein.
- iii) The intercellular components exposed to the outer solvent of the medium and the NPs entered directly inside the bacterial cell which ultimately results to the death of the cells of the organisms (Raffi *et al.*, 2008; Wu *et al.*, 2010). The changes in local electronic structure on the surface of very small size may lead to the antibacterial effects of NPs.

The possible mechanism found in this study based on the oxidation of lipids as shown in fig. 5. During photocatalytic activity of TiO_2 , oxygen is converted into hydrogen peroxide (H_2O_2) as given in equation 2 (Kikuchi *et al.*, 1997) produced H_2O_2 reacts with the O_2^- and form hydroxyl radical as shown in equation 3.



Cell wall is a barrier for bursting the cell whereas the plasma made up of lipids and proteins. The structure of cell wall damages due to the generation of oxidative stress by TiO_2 . The devastation of lipid of both *E. coli* and *S. aureus*, through oxidation is represented in fig. 5. Lipid of cell membrane constituents reacts with the reactive oxygen species (ROS) to form highly reactive lipid radical which with oxygen, converted into lipid peroxy radical that may react with proton to form lipid peroxide or react with the unreacted lipid molecule to form another lipid radical for chain reaction. Lipid peroxide on releasing hydroxyl ion converted into alkoxy radical that lead to cleavage into alkyl radical, aldehyde etc.

Furthermore, due to the presence of surplus carboxylic groups which when dissociated create negative charge on the cell due to which the overall cell charge on the cells of bacteria is negative. The Titanium NPs in solutions possess positive charge and electrostatic force of attraction between the opposite charges creates adhesion and biocidal effects observed (Baker *et al.*, 2005) subsequently in inhibition of microbial growth. Similar phenomenon of inhibition of bacterial growth observed in current investigation which is in accordance to the previous report of Tsuang *et al.*, (2008) who observed inhibition of *E. coli* through TiO₂ NPs for the infections due to the metal pins used for external support in orthopedic devices. In contrast to this, current study focuses on the usage of bactericidal activity of TiO₂ directly which may also be used for oral use as TiO₂ is edible compound and extensively used in pharmaceutical tablets as coatings. This will create new ways for microbiologists to study further and carried out testing on research mouse at laboratory scale.

Degradation of Acridine Orange

Acridine orange (AO), having vast medicinal applications and commonly found as main contaminates of water bodies. The water chemistry in current effort targeted a simple NPs based hygienic and efficient process for effective degradation of dye. Based on photo catalytic properties of simple (HPT) TiO₂ NPs, it was observed that effective dye degradation take place without adjusting pH which showed no role of H⁺ and OH⁻ ions. The spectral scan of the dye showed that dye degradation take place through complex formation where dye initially adsorbed on the surface then desorbed into smaller fragments (fig 6).

During the decolorization of AO solution, it was observed that the dye decomposed under the influence of TiO₂ without irradiation or temperature changes. The efficiency of the AO dye devastation was the consequences of diverse characteristics and contaminant eradication was achieved by photo catalytic properties of (HPT) NPs where 92% AO decolorized in 10 minutes. The degradation time depends upon the amount of TiO₂ where rapid degradation was observed at 0.5 g at a dye concentration of 30ppm. The recycled photo catalyst TiO₂ after 4 cycles retained the degradation efficiency of 75% against AO which was similar to the earlier reported work of Gautam *et al.*, (2016) who reported the reused efficiency of reported TiO₂ 83% and 71% for Methylene Blue (MB). The catalytic degradation of the AO was observed by degradation kinetics where 90% degradation efficiency of HPT anatase was recorded, which was greater with earlier reported work of Gautam *et al.*, (2016) who observed 88% degradation of anatase NPs in case of MB under short UV irradiation. The current results of HPT synthesised TiO₂ showed higher efficiency over previously published reports Chanathaworn *et al.*,

(2012) who reported 76.3% within 60 min for methylene green (MG) under UV irradiation while the current method involve no UV irradiation.

CONCLUSION

This study explores vast application of Titanium NPs in water chemistry with chemical and biological entities. The current investigation about antibacterial activity suggests that Titanium NPs can also be used in hospitals as well as in small clinics as a best antibacterial agent (for *E. coli* and *S. aureus*) for the safety of patients as Titanium is human friendly element. It was suggested that the current research requires further bacterial investigation to search additional field of application of Titanium NPs.

REFERENCES

- Al-Amin M, Dey SC, Rashid TU, Ashaduzzaman M and Shamsuddin SM (2016). Solar assisted photocatalytic degradation of reactive azo dyes in presence of anatase titanium dioxide. *Int. J. Latest Res. Eng. Technol.*, **2**(3): 14-21.
- Al-Harbi L, El-Mossalamy E, Arafa H, Al-Owais A and Shah M (2011). TiO₂ nanoparticles with tetra-pad shape prepared by an economical and safe route at very low temperature. *Mod. Appl. Sci.*, **5**(3): 130-135.
- Al-Taweel SS and Saud HR (2016). New route for synthesis of pure anatase TiO₂ nanoparticles via ultrasound-assisted sol-gel method. *J. Chem. Pharm. Res.*, **8**(2): 620-626.
- Ashiri R (2013). Detailed FT-IR spectroscopy characterization and thermal analysis of synthesis of barium titanate nanoscale particles through a newly developed process. *Vib. Spectrosc.*, **66**: 24-29.
- Baker C, Pradhan A, Pakstis L, Pochan DJ and Shah SI (2005). Synthesis and antibacterial properties of silver nanoparticles. *J. Nanosci. Nanotechnol.*, **5**(2): 244-249.
- Bhatia S (2016). Chapter: Nanoparticles types, classification, characterization, fabrication methods and drug delivery applications. Natural polymer drug delivery systems, Springer, pp.33-93.
- Chanathaworn J, Bunyakan C, Wiyaratn W and Chungsiriporn J (2012). Photocatalytic decolorization of basic dye by TiO₂ nanoparticle in photoreactor. *Songklanakarin J. Sci. Technol.*, **34**(2).
- Das TK, Couture M, Ouellet Y, Guertin M and Rousseau DL (2001). Simultaneous observation of the O—O and Fe—O₂ stretching modes in oxyhemoglobins. *Proc. Natl. Acad. Sci.*, **98**(2): 479-484.
- Desai VS and Kowshik M (2009). Antimicrobial activity of titanium dioxide nanoparticles synthesized by sol-gel technique. *Res. J. Microbiol.*, **4**(3): 97-103.
- Gautam A, Kshirsagar A, Biswas R, Banerjee S and Khanna PK (2016). Photodegradation of organic dyes

- based on anatase and rutile TiO₂ nanoparticles. *RSC Advances*, **6**(4): 2746-2759.
- Khan I, Saeed K and Khan I (2019). Nanoparticles: Properties, applications and toxicities. *Arabian J. Chem.*, **12**(7): 908-931.
- Kikuchi Y, Sunada K, Iyoda T, Hashimoto K and Fujishima A (1997). Photocatalytic bactericidal effect of TiO₂ thin films: dynamic view of the active oxygen species responsible for the effect. *J. Photochem. Photobiol. A: Chem.*, **106**(1-3): 51-56.
- Kim JS, Kuk E, Yu KN, Kim J-H, Park SJ, Lee HJ, Kim SH, Park YK, Park YH and Hwang C-Y (2007). Antimicrobial effects of silver nanoparticles. *Nanomed. Nanotechnol. Biol. Med.*, **3**(1): 95-101.
- Lee C, Kim JY, Lee WI, Nelson KL, Yoon J and Sedlak DL (2008). Bactericidal effect of zero-valent iron nanoparticles on *Escherichia coli*. *Environ. Sci. Technol.*, **42**(13): 4927-4933.
- Lin K-S, Chang N-B and Chuang T-D (2008). Fine structure characterization of zero-valent iron nanoparticles for decontamination of nitrites and nitrates in wastewater and groundwater. *Sci. Technol. Adv. Mater.*, **9**(2): 025015.
- Lin X, Li J, Ma S, Liu G, Yang K, Tong M and Lin D (2014). Toxicity of TiO₂ nanoparticles to *Escherichia coli*: effects of particle size, crystal phase and water chemistry. *PLoS One*, **9**(10): e110247.
- Mali SS, Kim H, Shim CS, Patil PS, Kim JH and Hong CK (2013). Surfactant free most probable TiO₂ nanostructures via hydrothermal and its dye sensitized solar cell properties. *Sci. Rep.*, **3**: 3004.
- Morones JR, Elechiguerra JL, Camacho A, Holt K, Kouri JB, Ramirez JT and Yacaman MJ (2005). The bactericidal effect of silver nanoparticles. *Nanotechnology*, **16**(10): 2346.
- Pathakoti K, Manubolu M and Hwang H-M (2019). Effect of Size and Crystalline Phase of TiO₂ Nanoparticles on Photocatalytic Inactivation of *Escherichia coli*. *J. Nanosci. Nanotechnol.*, **19**(12): 8172-8179.
- Peiris M, Guansekera T, Jayaweera P and Fernando S (2018). TiO₂ Nanoparticles from Baker's Yeast: A Potent Antimicrobial. *J. Microbiol. Biotechnol.*, **28**(10): 1664-1670.
- Qadri S, Ganoie A and Haik Y (2009). Removal and recovery of acridine orange from solutions by use of magnetic nanoparticles. *J. Hazard. Mater.*, **169**(1-3): 318-323.
- Raffi M, Hussain F, Bhatti T, Akhter J, Hameed A and Hasan M (2008). Antibacterial characterization of silver nanoparticles against *E. coli* ATCC-15224. *J. Mater. Sci. Technol.*, **24**(2): 192-196.
- Rosi H and Kalyanasundaram S (2018). Synthesis, characterization, structural and optical properties of titanium-dioxide nanoparticles using *Glycosmis cochinchinensis* Leaf extract and its photocatalytic evaluation and antimicrobial properties. *World News of Natural Sciences*, **17**: 1-15.
- Tsuang YH, Sun JS, Huang YC, Lu CH, Chang WHS and Wang CC (2008). Studies of photokilling of bacteria using titanium dioxide nanoparticles. *Artif. Organs*, **32**(2): 167-174.
- Vijayalakshmi R and Rajendran V (2012). Synthesis and characterization of nano-TiO₂ via different methods. *Arch. Appl. Sci. Res*, **4**(2): 1183-1190.
- Wu P, Imlay JA and Shang JK (2010). Mechanism of *Escherichia coli* inactivation on palladium-modified nitrogen-doped titanium dioxide. *Biomaterials*, **31**(29): 7526-7533.
- Zhang R, Zhang W, Bai X, Song X, Wang C, Gao X, Tian X and Liu F (2015). Discussion on the development of nano Ag/TiO₂ coating bracket and its antibacterial property and biocompatibility in orthodontic treatment. *Pak. J. Pharm. Sci.*, **28**(2 Suppl.): 807-810.